

## Resonance ionization in a gas cell: a feasibility study for a laser ion source

Z.N. Qamhieh, E. Vandeweert and R.E. Silverans

*Laboratorium voor Vaste Stof-Fysika en Magnetisme, K.U. Leuven, Celestijnenlaan 200 D, B-3001 Leuven, Belgium*

P. van Duppen, M. Huyse and L. Vermeeren

*Instituut voor Kern- en Stralingsfysica, K.U. Leuven, Celestijnenlaan 200 D, B-3001 Leuven, Belgium*

A laser ion source based on resonance photo-ionization in a gas cell is proposed. The gas cell, filled with helium, consists of a target chamber in which the recoil products are stopped and neutralized, and an ionization chamber where the atoms of interest are selectively ionized by the laser light. The extraction of the ions from the ionization chamber through the exit hole-skimmer setup is similar to the ion-guide system. The conditions to obtain an optimal system are given. The results of a two-step one-laser resonance photo-ionization of nickel and the first results of laser ionization in a helium buffer gas cell are presented.

### 1. Introduction

Experiments at on-line mass separators are often limited by isobaric contaminants present in the final beam. When fission reactions are used as the primary production mechanism, the production of exotic neutron-rich isotopes is overwhelmed by more stable isobars. Also beams of extreme neutron-deficient isotopes produced by heavy-ion induced reactions, suffer from the same problem.

The existence of this problem was already realized in the early days of on-line mass separators [1] and several possibilities to obtain chemical selectivity have been developed. By cooling for example the transfer line between the target and the ion source, one succeeded in producing very pure beams of noble gases, as has been shown at ISOLDE [2]. Another way to improve the selectivity of a catcher-ion source system is by making use of the fact that some elements are easily and some are hardly released from the catcher material. This method was used successfully at the GSI isotope separator [3]. However, these and other solutions are only applicable in very specific cases and give sometimes only a moderate reduction of the contaminants.

Resonance photo-ionization with lasers (further referred to as laser ionization) delivers in principle isotopically and isobarically pure ions because resonant excitation of the atoms is used. Providing the available lasers are suitable, it is possible to obtain an ionization efficiency near unity for about 80% of all elements, i.e. every atom that is irradiated by the laser will be ion-

ized [4]. In order to obtain this high efficiency, a relatively high laser power is needed, depending of course on the way the laser ionization is performed. So far only pulsed lasers can deliver this high power. These lasers have one major drawback, namely their low duty cycle ( $10^{-4}$ – $10^{-7}$ ). Since the production of the radioactive nuclei at many isotope separators, such as LISOL [5] is continuous, the maximum overall ionization efficiency will only be  $10^{-4}$ . Several ways have been proposed to solve this problem. The activity can be deposited on a surface with e.g. a He-jet system and can be desorbed with an ablating laser that works synchronously with the ionizing laser [6,7]. Or the activity can be stored in a moderately heated cavity preventing the atoms from condensation at the walls of the chamber. The low temperature limits the amount of surface ionization and a laser is sent in the chamber via a small exit hole [8]. In this article we propose a radically different method to overcome this low-duty cycle problem. Noble gases have the nice property of being able to store atoms as well as  $1+$  ions for a certain time. In other words, if one can store the atoms in between laser pulses in e.g. helium and extracting the ions out of the helium (as is done in the ion guide technique [9]), one has in principle an optimal system.

In this article, we will present the results of a feasibility study for a laser ion source at LISOL based on ionization in a gas cell (section 2). The ionization cross section of nickel using a one-laser system will be discussed in section 3 and the first test results of laser ionization in a gas cell filled with helium are presented in section 4.

## 2. Principle of the proposed laser ion source

We will first describe the laser ion source in general terms before giving some specific numbers on the dimensions of the chamber and the expected evacuation times. The problems related to diffusion losses will be addressed in a separate section.

### 2.1. Generalities of the laser ion source

A schematic drawing of how such a laser ion source might look like is shown in fig. 1. The recoil products from a fusion-evaporation reaction or fission reaction (only the former is shown in the figure for reasons of simplicity) are stopped in the helium gas of the target chamber and are transported together with the helium gas to the ionization chamber. The recoil products thermalize as neutrals or as  $1+$  charged ions, but after a few milliseconds (typically 2 ms) all the ions are neutralized [10]. If we make the transport time from the target chamber to the ionization chamber longer than the ion survival time, all the reaction products will be neutralized when they arrive in the ionization chamber. The short ion survival time is supposed to be due to recombination with the plasma electrons created by the projectile beam in the target chamber [11]. Especially in the case of heavy-ion induced reactions this effect is dramatic: the energy loss of e.g. an  $^{16}\text{O}$  (210 MeV) beam in helium is more than one order of magnitude higher than a 15 MeV proton beam. In the ionization chamber, the atoms of interest are selectively ionized by the laser light, while the other atoms are essentially unaffected. The ions are then transported by the helium flow through the exit hole behind which most of the helium is removed by the skimmer (differential pumping) and the ions are accelerated towards the analyzing magnet of the separator: a situation identical to the ion-guide system. Note that the primary beam does not pass the ionization chamber: this region is essentially free of plasma electrons and

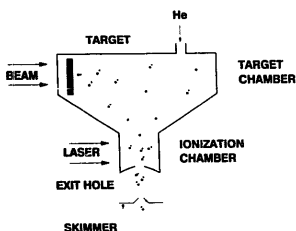


Fig. 1. Schematic layout of the laser ion source. The exit hole and skimmer are identical to those of the ion-guide system [10].

the ion-survival time against recombination with free electrons will become longer than  $\sim 10$  ms [11]. A process that has been neglected so far is the loss of ions and atoms due to diffusion to the walls of the target and/or ionization chambers. This problem will be addressed later.

By choosing the volume of the ionization chamber and the exit-hole diameter in such a way that the evacuation time ( $\tau_e$ ) of the ionization chamber equals the time between two laser pulses ( $\tau_{\text{rep}} = \nu_{\text{laser}}^{-1}$ ) and that  $\tau_e$  is smaller than the ion-survival time ( $\tau_{\text{ion}}$ ), one obtains an optimal system.

$$\tau_{\text{ion}} \geq \tau_e \geq \tau_{\text{rep}} \quad (1)$$

In this case every atom is irradiated at least once by the laser and every ion that is created will survive its transport to the exit hole. In order to stop recoil products from heavy-ion fusion evaporation reactions, pressures in the target chamber ( $P_{\text{t, ch}}$ , in mbar) higher than 500 mbar have to be used. This is a factor of 5 higher than in conventional ion-guide systems.

Because of the gas-load limit of the LISOL separator, currently  $Q_{\text{max}} = 100$  mbar l/s, we have to use an exit-hole diameter ( $Q_e$ ) of 0.7 mm. The proposed target chamber is 3 cm long and has a cross sectional area of  $1 \text{ cm}^2$ . The volume of the ionization chamber ( $V_{\text{ich}}$ , in  $\text{cm}^3$ ) is determined by the laser repetition rate:

$$V_{\text{ich}} = \tau_{\text{rep}} \frac{Q_{\text{max}}}{P_{\text{t, ch}}} \times 1000. \quad (2)$$

In the case of excimer lasers,  $\nu_{\text{laser}}$  is typically 200 Hz and consequently  $V_{\text{ich}} = 1 \text{ cm}^3$ ; in case of copper vapor lasers ( $\nu_{\text{laser}}$  around 10 kHz) and  $V_{\text{ich}} = 0.02 \text{ cm}^3$ . This means that the laser beam has to irradiate half a sphere around the exit hole with a radius of 0.78 cm (excimer laser) or 0.21 cm (copper vapor laser) depending on the type of laser used. Here we assume that the helium flow inside the target and ionization chambers is homogeneous. In order to make sure that the transport time between the target and the ionization chambers is longer than  $\sim 5$  ms – all ions must be neutralized – we have to insert an additional volume in between these two chambers. The total evacuation time of the laser ion source will then be about 23 ms in the case of an excimer laser and about 19 ms in the case of a copper vapor laser. Consequently, nuclei with a half-life shorter than  $\sim 30$  ms will suffer to a certain extent from decay losses in the laser ion source.

Another process that causes a reduction of the overall efficiency of the laser ion source is the formation of molecules by the recoil products combining with impurity atoms. Furthermore, when a recoil atom thermalizes in a metastable state while the laser frequency is tuned to ionize the ground state atoms, it will be unaffected by the laser light. Both processes can only be studied on line; so far this has not been performed.

## 2.2. Diffusion losses in the laser ion source

In order to get an idea of the losses due to diffusion to the walls of the chamber, one can consider the following. Since in the target chamber a fraction of the helium atoms are ionized by the impact of the primary beam, one can use the ambipolar interdiffusion of recoil ions through a different but ionized medium. An average value for this diffusion coefficient ( $D_a$  in  $\text{cm}^2/\text{s}$ ) for all ions in helium at room temperature is given by [12]:

$$D_a = 650/P_{i,\text{ch}}. \quad (3)$$

With this diffusion coefficient one can solve the diffusion equation inside a sphere or a cylinder to get an idea of the spreading out of the ions in the target chamber. After a time  $\tau$  [s],  $1/e$  of the ions have diffused over a distance  $X$  [cm],  $X$  and  $\tau$  are related as follows:

$$\tau = \frac{1}{D_a} \left( \frac{X}{2.4} \right)^2. \quad (4)$$

At a pressure of 500 mbar, the ions diffuse over a mean distance of  $\sim 3$  mm in about 20 ms. If the evacuation of the chamber are homogeneous, then the losses due to diffusion to the walls of the chamber are small. However, using lower pressures might cause

significant losses. This was evidenced by efficiency measurements for the ion-guide system using recoil products from  $\alpha$ -decaying nuclei [5]. The efficiency measured as a function of pressure rises when going to higher pressures and seems to saturate at 175 mbar. This effect is interpreted as being due to diffusion losses since the diffusion coefficient is inversely proportional to pressure (see eq. (3)).

On the other hand, if a preferential flow regime exists inside the target and ionization chambers, then part of the gas cell will be evacuated much faster and the diffusion process has to be re-examined in view of these flow patterns. Unfortunately, this information is not yet available.

## 3. Selective two-step photo-ionization

Because of the strong nuclear physics interest in the study of neutron-deficient nickel isotopes – approaching the double magic nucleus  $^{78}\text{Ni}$  – we started to study the photo-ionization of nickel. Other elements like manganese, cobalt, molybdenum and barium have also been investigated. For the laser ionization, we used the two-step one-color photo-ionization technique which was first used by Ambartsumyan et al. [13]. A full discussion of this technique can be found in ref. [4].

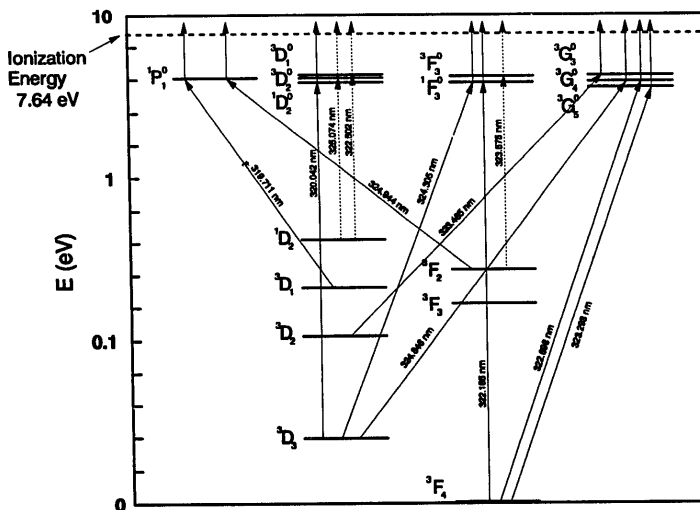


Fig. 2. Part of the atomic level scheme of nickel. All tabulated lines in the wavelength region 319–326 nm [14] are shown. The dashed lines were not observed in this study.

Two identical photons are subsequently absorbed by the nickel atom (fig. 2): resonant absorption of the first photon excites the nickel atom to a level above half the ionization limit, the excited atom is then ionized by absorbing a second identical photon. At sufficiently high photon flux and fluence, the excitation step can be saturated [4]. Consequently, the number of ions ( $N_1$ ) detected per laser pulse can be expressed as a function of the laser fluence ( $\Phi$  in photons/cm<sup>2</sup>). In the case of an ideal, two-level system this becomes:

$$N_1 = N_0[1 - \exp(-\sigma_1\Phi/2)], \quad (5)$$

where  $\sigma_1$  is the photo-ionization cross section of the excited state in units of cm<sup>2</sup> and  $N_0$  is the total number of the initial state atoms irradiated with the ionizing laser beam. This equation will be used for the determination of  $\sigma_1$ .

### 3.1. The experimental setup

The second harmonic (532 nm) output of a Q-switched Nd:YAG (Quanta-Ray DCR-11) pulsed laser was used to pump a (Quanta-Ray PDL-3) dye laser with a DCM solution in methanol. Frequency doubling using a wavelength extender (Quanta-Ray WEX-1) resulted in UV laser light tunable over the 310–330 nm wavelength region. The power of the laser beam was measured using a calibrated thermopile. This thermopile was also used in combination with a movable knife edge, intersecting the laser beam, to measure its cross sectional area. The 320 nm laser beam of 10 Hz repetition rate, about 10 ns pulse duration time, 4 (1) mm<sup>2</sup> cross section area, and 3.5 mJ per pulse maximum energy was directed towards a vacuum chamber ( $10^{-6}$ – $10^{-5}$  mbar) in which the nickel atoms were produced by resistive heating of a nickel wire of 1 mm diameter. As a result of the interaction between the laser beam and part of the created atoms, ions were produced. These ions were collected on a negatively biased detector.

### 3.2. Results

Scanning the laser in the wavelength region 320–325 nm while keeping the temperature of the nickel wire at about 1270 K, approximately all tabulated spectral lines of nickel [14] in addition to several nontabulated ones were observed (table 1 and fig. 2). The experimental resonance ionization spectrum is presented in fig. 3. The strongest ground-state originating transition at 322.698 nm was chosen to measure the photo-ionization cross section ( $\sigma_1$ ) of the <sup>3</sup>G<sub>4</sub> excited state of nickel. During the measurement, the temperature of the nickel wire was kept constant while the fluence ( $\Phi$ ) of the ionizing laser was varied. The resulting resonant signal ( $N_1$ ) as a function of energy was fitted using eq.

Table 1

Transitions observed for nickel and their relative intensity. The temperature of the nickel wire was 1270 K and the laser energy 2.1 mJ per pulse. The intensity is normalized to the strongest transition (322.698 nm). The transitions labelled with 1 start from the <sup>3</sup>F<sub>4</sub> ground state, 2 from <sup>3</sup>D<sub>3</sub>, 3 from <sup>3</sup>D<sub>2</sub>, 4 from <sup>3</sup>D<sub>1</sub>, 5 from <sup>3</sup>F<sub>2</sub>, 6 from <sup>1</sup>D<sub>2</sub> [14]. And those labelled with \* are not tabulated in the same reference.

Label	Wavelength [nm]	Relative intensity <sup>a</sup>
4	319.711	0.01
2	320.042	0.04
*	321.695	0.01
1	322.165	0.02
*	322.355	0.01
6	322.502	<sup>b</sup>
1	322.698	1.00
1	323.293	0.80
3	323.465	0.03
5	323.575	<sup>b</sup>
*	323.610	0.04
*	323.688	0.01
*	324.150	0.06
2	324.305	0.48
*	324.680	0.05
*	324.769	0.06
2	324.846	0.60
5	324.944	0.02
6	325.074	<sup>b</sup>

<sup>a</sup> Error on the relative intensity is 0.01.

<sup>b</sup> Not observed in this study.

(5) (fig. 4) and the obtained value for  $\sigma_1$  is  $6.3(30) \times 10^{-17}$  cm<sup>2</sup>. The large error reflects the uncertainty on the power reading and on the determination of the cross sectional area of the laser beam. Note that the

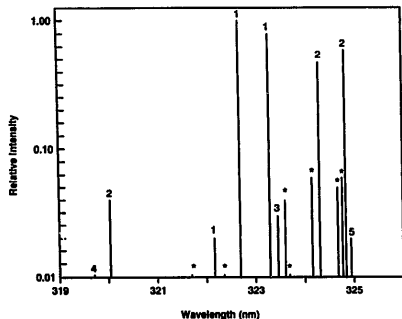


Fig. 3. Resonance ionization spectrum for nickel. For the experimental conditions and the meaning of the symbols used, see the caption of table 1 above.

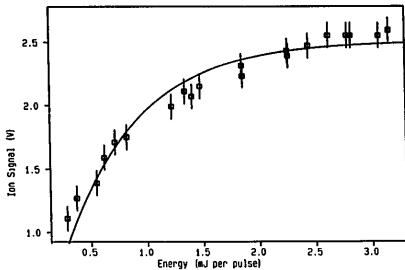


Fig. 4. Ion signal vs laser energy per pulse. The curve is the result of a fit with the data using eq. (5).

ionization step was almost completely saturated (see Fig. 4), i.e. approximately all nickel atoms irradiated by the laser were ionized.

For laser ionization, instead of using two-step one-laser photoionization, one can use two or more lasers to resonantly excite the atoms to high-lying states for which the ionization cross section can be much higher. Eventually, the atom can be excited in an auto-ionizing state. This will enhance  $\sigma_1$  by two or more orders of magnitude. Consequently, the necessary laser power can be reduced to the same extent but at the cost of using two or more laser systems. This will make the stabilization of the complete laser setup more cumbersome and might induce problems for long term experiments where one needs a stable beam for a few days.

#### 4. Photo-ionization in a gas cell

In order to investigate the performances of the ionization chamber of the proposed laser ion source (Fig. 1), we studied photo-ionization in a gas cell similar to the ionization chamber. A schematic drawing of this cell is shown in Fig. 5. The atoms of interest are created

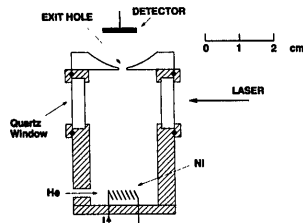


Fig. 5. Schematic drawing of the gas cell used for testing the resonant ionization in a buffer gas.

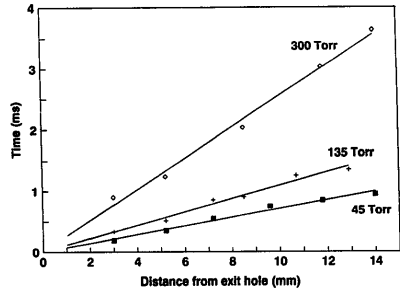


Fig. 6. The time elapsed between the moment of impact of the laser beam and the moment the ions are detected as a function of the distance ( $d$  in mm) between the position of the laser beam and the exit hole ( $\varnothing_{\text{exit}} = 1.0$  mm). The laser beam was moved in a direction parallel to the central axis of the gas cell.

by heating a nickel or molybdenum filament that surrounds a small piece of material. The filament is situated at the place where the helium gas enters the chamber. The created atoms flow together with the helium towards the exit hole. In the region just in front of the exit hole, where the laser beam perpendicular to the central axis of the cell can enter and leave the gas cell through two quartz windows, the atoms are ionized. Once the ions have crossed the exit hole, they are collected on a negatively biased plate. In this setup we measure the amplitude of the ion signal and the time elapsed between the moment of impact of the laser beam and the moment the ions are detected. The flight time between the exit hole and the detector is considered to be negligible. Fig. 6 shows the time ( $t$  in ms) as a function of the distance ( $d$  in mm) between the position of the laser beam and the exit hole ( $\varnothing_{\text{exit}} = 1.0$  mm). The laser beam is moved in a direction parallel to the central axis of the gas cell. If we assume that the gas cell is evacuated in a homogeneous way we can calculate from simple principles the time it takes for an ion formed at a distance  $d$  from the exit hole to be evacuated from the cell. The conductance of the exit hole can be written as a function of the exit-hole diameter ( $\varnothing_{\text{exit}}$  in mm):  $C_{\text{exit}} = 0.45(\varnothing_{\text{exit}})^2$  in l/s. The evacuated volume is a function of  $d$  and of the cross sectional area of the gas cell. Consequently, the expression for  $t$  becomes  $t = 0.70d/(\varnothing_{\text{exit}})^2$ . One notices that the ions are evacuated much faster than expected; at  $d = 10$  mm the time is expected to be 7 ms while from the experiment one obtains about 3 ms. In addition, one notes that the evacuation time depends on the pressure, although this is not expected in this pressure regime where the conductance ( $C_{\text{exit}}$ ) should be inde-

pendent of the pressure. When moving the laser beam away from the central axis while keeping the distance relative to the exit hole fixed, one notices a strong increase in the evacuation time for ions that are created away from the central axis of the gas cell: preferential flow patterns seem to exist inside the gas cell. These results are confirmed by a recent study of the evacuation of ionized recoil products from the  $\alpha$  decay of  $^{223}\text{Ra}$  inside the ion-guide system [5]. The existence of preferential flow patterns inside the gas cell and also inside the ion-guide system might force us to modify the design of our laser ion source and to use lasers with a high repetition rate, e.g. copper vapor lasers. On the other hand, this can also give some interesting new possibilities: the laser beam might be injected on to the central axis of the gas cell, the delay time of the laser ion source will be considerably smaller, diffusion losses out of the preferential flow channels can be neglected, etc. This investigation is still in progress.

## 5. Conclusion

In this paper, we described the possible layout of a laser ion source based on resonance photo-ionization in a gas cell. Hereby, the problems related to the low duty cycle of pulsed laser systems – that have to be used for efficient laser ionization – are dealt with by storing the atoms of interest between laser pulses in a cell filled with noble gas (helium). The only condition that has to be fulfilled is an equality between the inverse of the laser repetition rate, the evacuation time of the ionization chamber and the ion survival time. We have studied the ionization of nickel atoms using the two-step one-color photoionization technique. Even in this unfavorable condition – the ionization cross section using more than one excitation step is two or more orders of magnitude higher – ionization efficiencies near unity can be obtained with commercially available laser systems. The measurements in a gas cell similar to the ion-guide system seem to indicate that inside such a cell preferential flow regimes exist. These flow patterns will be further investigated by laser ionization in a gas cell as well as with the ion-guide system, because they will finally determine the design of the laser ion source and the choice of lasers to be used (high or moderate repetition rate).

## Note added in proof

Recent measurements of the evacuation times, taken with an improved pumping system, showed that small leaks were present in the gas cell. After repairing this gas cell, the pressure dependence of the evacuation times (fig. 6) was no longer observed, but the measured values were still much shorter than expected from conductance calculations.

## Acknowledgements

This work was supported by the Interuniversitair Instituut voor Kernwetenschappen and Fonds voor Kollektief Fundamenteel Onderzoek, Belgium.

## References

- [1] H.L. Ravn and B.W. Allardyce, On-line mass separators, in: *Treatise on Heavy-Ion Science*, vol. 8, ed. D.A. Bromley (Plenum, New York, 1989).
- [2] H.L. Ravn, *Phys. Rep.* 54 (1979) 201.
- [3] R. Kirchner, O. Klepper, D. Marx, G.E. Rathke and B. Sherrill, *Nucl. Instr. and Meth.* A247 (1986) 265.
- [4] G.S. Hurst and M.G. Payne, *Principles and Applications of Resonance Ionization Spectroscopy* (IOP Publishing, 1988).
- [5] M. Huysse et al., these Proceedings (EMIS-12), *Nucl. Instr. and Meth.* B70 (1992) 50.
- [6] J.K.P. Lee, J.E. Crawford, V. Raut, G. Savard, G. Thekkadath, T.H. Duong and J. Pinard, *Nucl. Instr. and Meth.* B26 (1987) 444.
- [7] W.M. Fairbank and H.K. Carter, *Nucl. Instr. and Meth.* B26 (1987) 357.
- [8] F. Ames, T. Brumm, K. Jager, B.M. Suri, H. Rimke, N. Trautmann and R. Kirchner, *Appl. Phys.* B51 (1990) 200.
- [9] J. Arje, *Phys. Scripta* T3 (1983) 37.
- [10] K. Deneffe, B. Brijs, E. Coenen, J. Gentens, M. Huysse, P. Van Duppen and D. Wouters, *Nucl. Instr. and Meth.* B26 (1987) 399.
- [11] P. Taskinen, H. Penttillä, J. Aystö, P. Dendooven, P. Jauho, A. Jokinen and M. Yoshii, *Nucl. Instr. and Meth.* A281 (1989) 539.
- [12] M.A. Biondi and S.C. Brown, *Phys. Rev.* 75 (1949) 1700.
- [13] R.V. Ambartsumyan, A.M. Apatin, V.S. Letokhov, A.A. Makarov, V.I. Mishin, A.A. Puretskii and N.P. Furzikov, *Sov. Phys. JETP* 43 (1976) 866.
- [14] W.L. Wiese and A. Musgrave, National Institute for Standards and Technology, *Spectroscopic Data for Titanium, Chromium and Nickel*, Oak Ridge National Laboratory, 3 Nickel (1989).